Pindari cold water pollution: pneumatic assessment

WRL TR 2024/27, November 2024

By D M Gilbert, F C Chaaya and B M Miller

UNSW
Water Research
Laboratory

UNSW
SYDNEY

UNSW
Water Research
Laboratory

UNSW
SYDNEY

Pindari cold water pollution: pneumatic assessment

WRL TR 2024/27, November 2024

By D M Gilbert, F C Chaaya and B M Miller

Project details

Report title	Pindari cold water pollution: pneumatic assessment
Authors(s)	D M Gilbert, F C Chaaya and B M Miller
Report no.	2024/27
Report status	Final
Date of issue	November 2024
WRL project no.	2022050
Project manager	D M Gilbert
Client	NSW Department of Primary Industries and Regional Development – Fisheries
Client address	1243 Bruxner Highway Wollongbar NSW 2477
Client contact	Matthew Gordos matthew.gordos@dpi.nsw.gov.au
Client reference	#

Document status

Version	Reviewed by	Approved by	Date issued
Draft	BMM, FCC	FF	13/11/24
Final	BMM, FCC	FF	14/11/24

This report should be cited as: Gilbert, DM, Chaaya, FC & Miller, BM 2024, Pindari cold water pollution: pneumatic assessment, WRL Technical Report 2024/27, UNSW Water Research Laboratory.

UNSW
Water Research
Laboratory

www.wrl.unsw.edu.au
110 King St Manly Vale NSW 2093 Australia
Tel +61 (2) 8071 9800 ABN 57 195 873 179

Contents

List of tables

List of figures

1 Introduction

Cold water pollution is a complex issue with a range of ecological, environmental and social impacts caused by the release of cold water from dams. This issue affects many large storage dams throughout NSW, especially where thermal stratification drives large temperature differences within the reservoirs. An international literature review undertaken by UNSW Water Research Laboratory (WRL) investigated the causes and impacts of, and options for mitigating cold water pollution (Chaaya and Miller, 2022). This review identified artificial destratification via bubble plumes as the only feasible mitigation option capable of addressing both cold water pollution and other water quality issues caused by reservoir stratification in a range of reservoir sizes. The successful application of bubble plume destratification in large storage reservoirs was found to be limited, primarily due to the significant operational costs at larger scales resulting in under-designed systems. As such, understanding the pneumatic processes in order to optimise the bubble plume diffuser design is considered necessary for a feasible and efficient artificial destratification system.

Given the limited work that has been undertaken previously to optimise design and operation of these systems, and limited successful operations in larger reservoirs historically, a pilot trial destratification system was recommended to demonstrate feasibility. WRL was previously engaged by the NSW Department of Primary Industry and Regional Development – Fisheries (DPIRD Fisheries) to identify the most appropriate NSW dam in which to install and operate a trial destratification system. Pindari Dam located on the Severn River, (identified as one of the eight high-priority dams in NSW; NSW Cold Water Pollution Interagency Group, 2012), was deemed the most appropriate. WRL was then engaged by DPIRD Fisheries to undertake tasks to support the design of the proposed Pindari Dam bubble plume artificial destratification trials, summarised in the following reports:

- WRL TR2022/04 Pindari dam – mitigating cold water pollution through artificial destratification (Chaaya and Miller, 2023a)
- WRL TR2022/19 Pindari Dam cold water pollution mitigation through artificial destratification – Monitoring network recommendations (Chaaya and Miller, 2023b)
- WRL TR2023/05 Pindari destratification trial - conceptual design details (Chaaya and Miller, 2024a)
- WRL TR2024/05 Pindari destratification – numerical modelling of operational procedures to balance power requirements (Chaaya and Miller, 2024b)

This report presents laboratory testing of pneumatic air flow into a water column through various diffuser port sizes. This testing was designed to be general in nature and capture the likely range of conditions encountered in bubble plume diffuser design, extending beyond Pindari. However, the impacts to the Pindari Dam diffuser design are explicitly discussed.

- Section 2 details the experimental method
- Section 3 provides results, verifying the existing theory on pneumatic air flow and establishing the value and variability of the coefficient of discharge (a key design parameter)
    - The existing theory was found to fit experimental data very well ($R^2 = 0.995$)
    - The coefficient of discharge was found to be 0.68 ± 0.05
- Section 4 then discusses the implication of the experimental findings on the Pindari Dam bubble plume diffuser design (and bubble plume diffuser design more broadly)
    - The use of more efficient nozzles is not recommended
    - The measured variability does not significantly impact the Pindari diffuser design

2 Experimental methods

2.1 Theoretical flow through an orifice plate

The flow of compressed air through a diffuser port can be idealised as the flow of a compressible fluid through an orifice, which is theoretically well understood. This relationship does not account for the two-phase mixing of air and water just above the diffuser port, assuming a single phase (compressed air). This experiment checks that this simplification is appropriate and applicable for the design of a destratification diffuser.

There are two flow conditions that can occur as a compressible fluid (like compressed air) passes through an orifice: subcritical flow or supercritical flow. The flow state depends on the ratio of the internal and external pressures around the diffuser. Flow can be considered subcritical (FEMA, DOT & EPA, 1989) when:

$$\frac{P_{\text{ext}}}{P_{\text{int}}} \leq \left(\frac{2}{\gamma+1}\right)^{\frac{\gamma}{\gamma-1}} = 0.528 \quad (\text{for compressed air}) \tag{1}$$

$$\text{or } P_{\text{int}} \leq 1.9 P_{\text{ext}}$$

This means that the flow will be subcritical unless the absolute pressure inside the pipeline is approximately twice the absolute pressure outside the pipeline. Based on the realistic range of pressures and air flow rates, it is not anticipated that supercritical flow conditions will occur in bubble plume destratification systems, hence these experiments only include subcritical flow conditions. For subcritical flow conditions, a mechanical energy balance is typically used (FEMA, DOT & EPA, 1989; Lewis et al., 1991) to calculate the flow through an orifice as:

$$Q_n = \frac{CA}{\rho_{atm}} \sqrt{2\rho_{\text{int}} P_{\text{int}} \left(\frac{\gamma}{\gamma-1}\right)\left[\left(\frac{P_{\text{ext}}}{P_{\text{int}}}\right)^{\frac{2}{\gamma}} - \left(\frac{P_{ext}}{P_{\text{int}}}\right)^{\frac{\gamma+1}{\gamma}}\right]} \tag{2}$$

$$\rho_{\text{int}} = \frac{P_{\text{int}}}{R_{\text{specific}} T_{\text{int}}}$$

Where:

Q_n = Flow rate through the orifice under atmospheric conditions (1 atmosphere and 20 °C), m_n^3/s
ρ_{atm} = Air density at atmospheric conditions (ρ_n = 1.19 kg/m^3 at 1 atmosphere and 20 °C)
C = Coefficient of discharge, unitless
A = Area of orifice, m^2
ρ_{int} = Air density at the orifice, inside the diffuser, kg/m^3
γ = Heat capacity ratio ($\gamma = 1.4$ for air), unitless
P_{int} = Absolute pressure at the orifice, inside the diffuser, Pa
P_{ext} = Absolute pressure outside the orifice (hydrostatic pressure from water depth), Pa
R_{specific} = Specific gas constant, R = 287.1 J/Kg
T_{int} = Temperature inside the diffuser, °K

2.2 Experimental setup

2.2.1 Pressure chamber

A custom experimental rig was constructed at the UNSW Water Research Laboratory (WRL) for these trials, as shown in Figure 1 and Figure 2. Air was pumped into the bottom chamber at a pressure set by the regulator, which then discharged up into the top chamber through interchangeable 20 mm thick high density polyethylene (HDPE) plates with different hole sizes. The top chamber was half filled with water and pressurised to a level controlled by the adjustable back pressure relieving valve. The pressure on either side of the HDPE plate, the flowrate and the temperature were all measured. The pressure sensors were installed in the pipe flange, 50 mm above and below the HDPE plate. Both the top and bottom chamber were constructed from pressure rated PVC pipe, with acrylic windows installed into the top chamber to allow for visual observations.

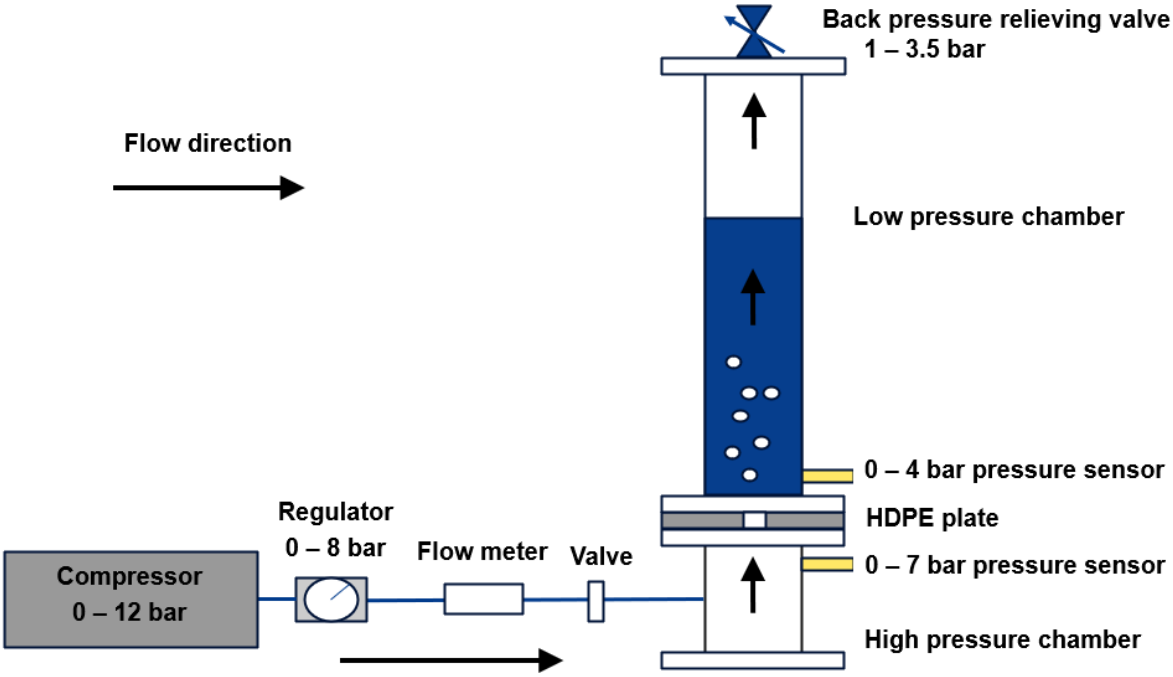

Figure 1 Schematic of experimental setup

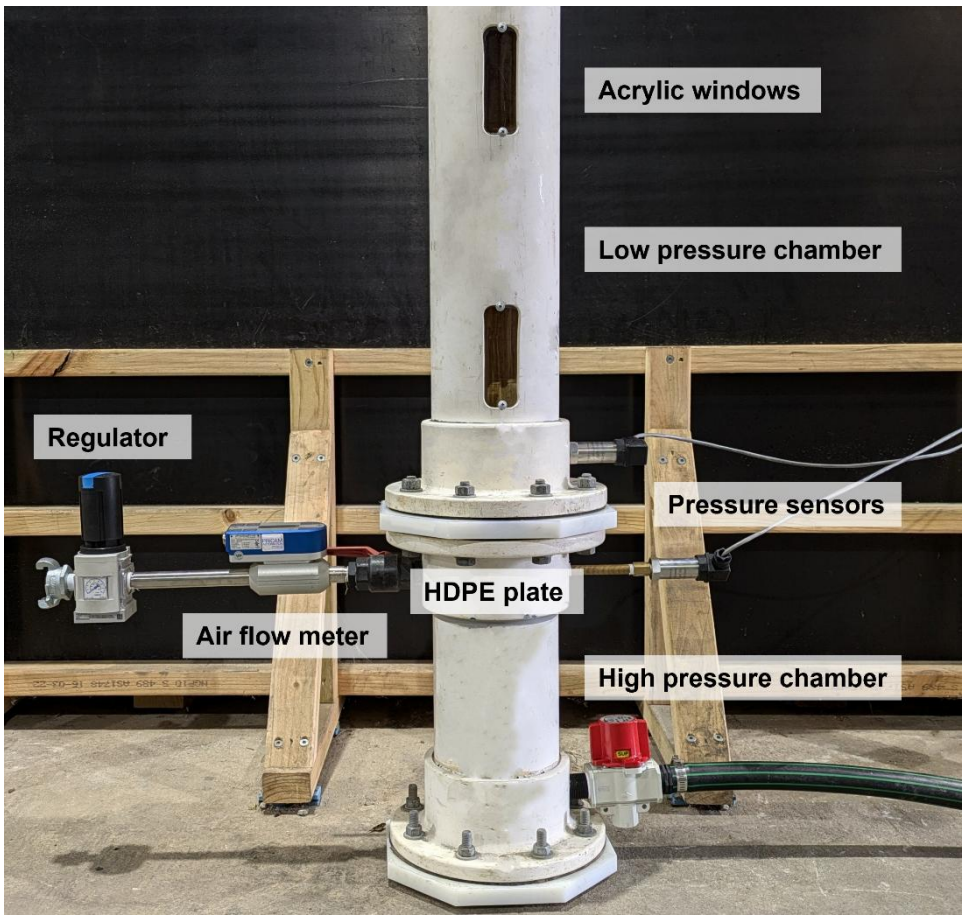

Figure 2 Photograph of lower chamber of the experimental setup

2.2.2 Diffuser port diameters

Different diffuser port diameters were tested by swapping out the HDPE plate separating the top and bottom chambers (Figure 1 and Figure 2). A summary of the configurations tested has been provided in Table 1. A 20 mm thick HDPE plate was used to match the proposed Pindari diffuser pipeline at the time of experimentation. A range of sizes from 1.5 to 7 mm was selected based on previous bubble plume destratification systems and WRL's recommended design.

Holes were labelled "clean" (Table 1) when constructed using a drill press and cleaned of any burrs. A single hole was drilled for most tests, however in some instances, multiple holes were used to ensure a flow rate that could be accurately measured by the flow meter.

Two additional tests were also conducted with "burred" holes. Holes for these tests were drilled using a cordless drill, aiming to represent the conditions of the actual diffuser construction. Burrs were not removed before testing and a comparison between the burred and clean holes has been provided in Figure 3. An initial burred test (S3) was conducted with a single burred 3 mm hole and then a second test (S4) was conducted with five 3 mm burred holes to account for the variability of hand drilled holes. The five holes were arranged in a square pattern with 40 mm spacing and an additional hole in the centre.

During preliminary testing, it was noticed that the as constructed port diameter did not exactly match the diameter of the drill bit used, despite the use of precision drill bits. This was found to have a significant

impact on the results (discussed in Section 4.4.2), especially for the smaller holes, and thus the as constructed diameter was measured to an accuracy of ± 0.05 mm.

Table 1 Diffuser hole size scenarios

Scenario ID	Number of tests	Nominal diameter (mm)	As constructed diameter (mm)	Number of holes	Description
S1	11	1.5	1.4	4	Clean
S2	10	3.0	2.8	1	Clean
S3	9	3.0	3.2	1	Burred
S4	11	3.0	2.9	5	Burred
S5	12	5.0	4.9	1	Clean
S6	9	7.0	7.0	1	Clean

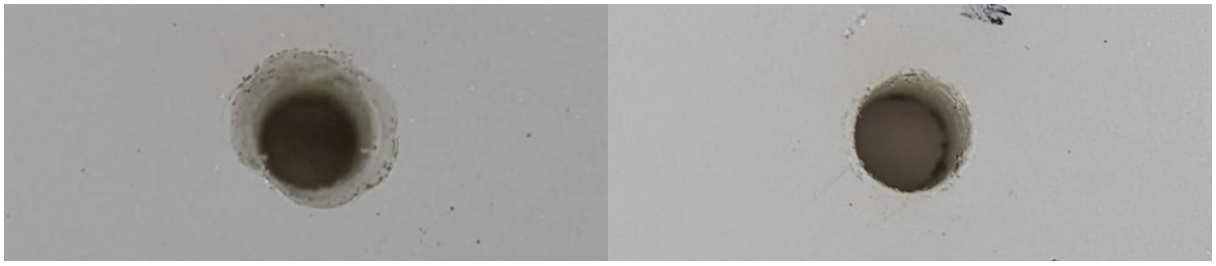

Figure 3 Burred 3.1 mm hole (left) and clean 2.8 mm hole (right)

2.2.3 Quality assurance

Prior to testing each scenario the chamber was assembled and pressurised to the maximum pressure for that scenario. The flow meter was used to monitor for any air leaks over a 10 minute period. Soapy water was also brushed onto the bolts, tappings and flanges to identify and locate any leaks. During this period, the pressure in the top and bottom chamber was at equilibrium, allowing for the two pressure sensors to be compared for any discrepancies. Pressure readings were also compared to the pressure sensor in the flow meter as an additional quality check. The instruments used to measure each parameter are shown in Table 2. The flow meter and pressure transmitters were factory calibrated.

Table 2 Instrumentation range and accuracy

Parameter	Instrument	Range	Accuracy
Flow	VP Flowscope	0 – 22 L_n/s	± 0.1 L_n/s
Temperature	VP Flowscope	0 – 80 ^oC	± 0.1 ^oC
Pressure	MRB20 pressure transmitter	0 – 4 bar	± 0.0012 bar
Pressure	MRB20 pressure transmitter	0 – 7 bar	± 0.0007 bar
Area	Telescopic bore gauges and micrometer	1 – 10 mm	± 0.05 mm

Note: L_n/s is the airflow rate under normal atmospheric conditions (1 atmosphere and 20 ^oC)

3 Results

3.1 Overview

A total of six scenarios and 62 tests were completed as part of this experiment, with complete results shown in Table A-1. A coefficient of discharge of **C = 0.68** was found to provide the lowest root mean square error between flow calculated using Equation (2) and measured flow, with a plot of the fit shown in Figure 4. The theoretical equation was found to fit the measured data very well, with an R^2 of 0.995.

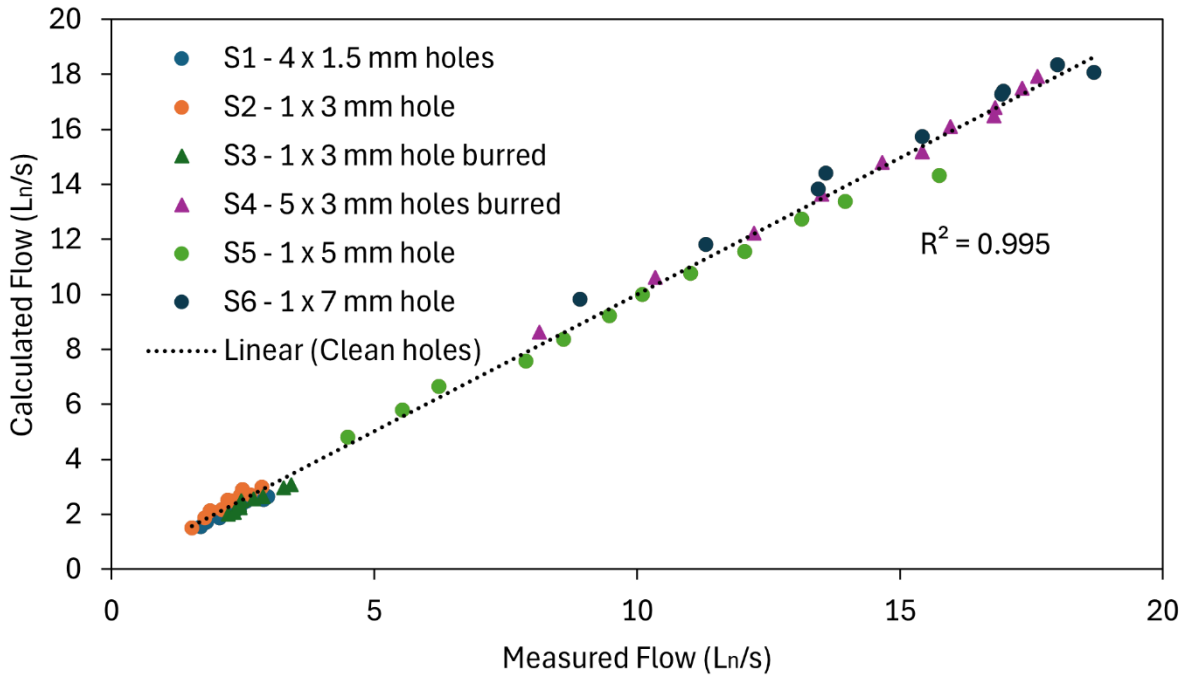

Figure 4 Calculated vs measured flow for a coefficient of discharge of C = 0.68. Hole diameters in the legend are nominal, calculations were done with as-constructed values

3.2 Variability of coefficient of discharge

Two sources of variability in the determined coefficient of discharge were identified during testing. The first was the hole diameter, which was measured to an accuracy of ± 0.05 mm. The theoretical equation (2) takes the form $Q = CA \times [\text{pressure and temperature terms}]$ meaning that, when fitting a coefficient value, the coefficient (C) is linearly related to area and quadratically related to diameter. As such, there was more uncertainty for the smaller diameter holes, as indicated in Table 3.

The other source of variability was the standard deviation across the roughly 10 tests undertaken for each scenario. This variability was relatively consistent across the scenarios, with a median value of ± 0.03. The mean coefficient of discharge and total variance for each scenario has been plotted in Figure 5. A slight decrease in coefficient of discharge with increasing hole diameter was observed, but this was not statistically significant (P > 0.05).

Table 3 Variability of coefficient of discharge (C)

Scenario ID	As constructed hole size (mm)	Mean coefficient of discharge	Variance with area	Variance with standard deviation	Total variance
S1	1.4	0.73	± 0.05	± 0.03	± 0.08
S2	2.8	0.63	± 0.03	± 0.03	± 0.06
S3	3.1	0.69	± 0.03	± 0.03	± 0.06
S4	2.9	0.67	± 0.02	± 0.01	± 0.03
S5	4.9	0.69	± 0.02	± 0.03	± 0.05
S6	7	0.66	± 0.01	± 0.02	± 0.03

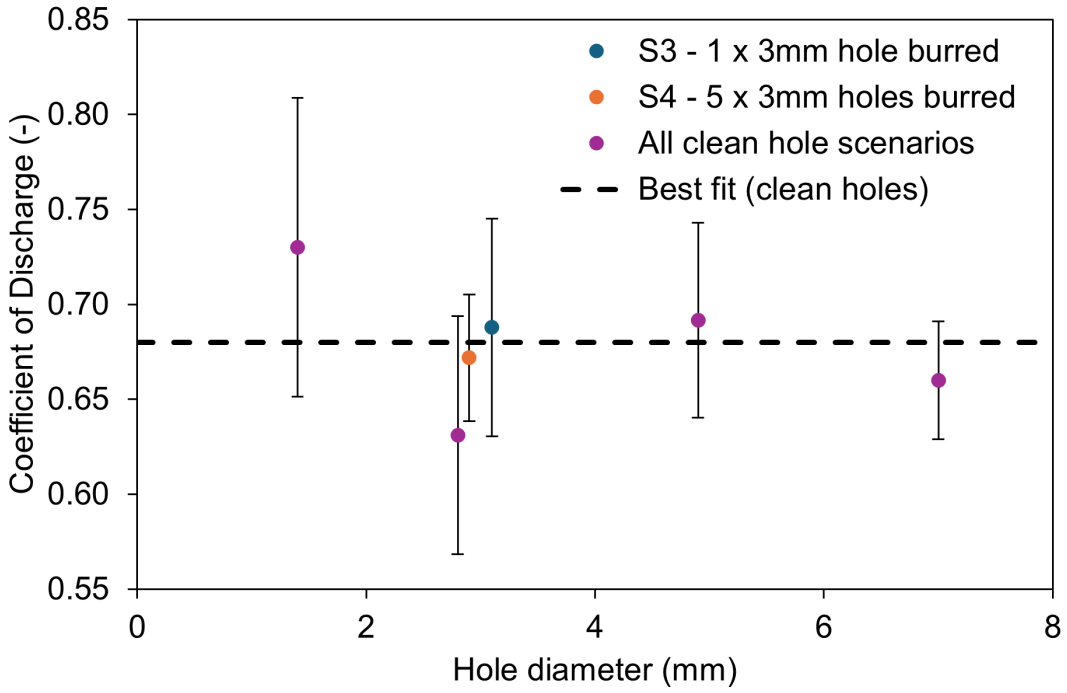

Figure 5 Variation in optimal coefficient of discharge across each scenario. Error bars denote range in calculated coefficient value across each test and with uncertainty due to diameter measurement. Nominal hole diameter is indicated in the legend.

4 Implications for Pindari diffuser design

4.1 Preamble

This section discusses the implications of the experimental findings on the design of the Pindari destratification system diffuser. The diffuser design has been through several iterations, but the consideration in this report is the design provided by WRL to DPIRD Fisheries in a letter dated 27 August 2024 as follows:

- 500 m diffuser length
- 100 mm ID pipeline
- Maximum water depth of 69 m
- 20 source clusters (groups of ports) each spaced 25 m apart
- 110 total ports
- 5 mm port diameter
- First 10 source clusters comprised of 5 x 5 mm ports at 100 mm spacing
- Second 10 source clusters comprised of 6 x 5 mm ports at 100 mm spacing

4.2 Methodology for diffuser calculations

The required compressor pressure and airflow distribution along a specified diffuser pipeline has been calculated using a spreadsheet tool developed by WRL. The methodology for this tool was derived from Lewis et al., (1991) and is summarised here:

1. Define the inputs: total free air flow rate, depth of water above the diffuser, and the port diameters and layout (number per cluster, distance between clusters)
2. Calculate the losses along the initial length of the pipeline, before the first source cluster. This is calculated using Equation (3)
3. Calculate the flow through a source cluster according to Equation (2) (validated in this study)
4. Subtract the flow through the source cluster from the current free air flow rate in the pipeline
5. Calculate the pressure recharge according to Equation (4), this is a small adjustment generated by the decrease in flow velocity across the holes as air is discharged into the water storage (Lewis et al., 1991)
6. Add the pressure recharge back to the pressure at this point in the pipeline
7. Calculate the losses along the pipeline between source clusters using Equation (3) and update the pressure at this point in the diffuser pipeline
8. Repeat steps 3 to 7 until the end of the diffuser pipeline is reached
9. Iterate through different compressor pressure values until the sum of airflow through the source clusters matches the specified total free air flow rate

$$Q_n = \frac{CA}{\rho_{atm}} \sqrt{2\rho_{\text{int}} P_{\text{int}} \left(\frac{\gamma}{\gamma - 1}\right) \left[\left(\frac{P_{\text{ext}}}{P_{\text{int}}}\right)^{\frac{2}{\gamma}} - \left(\frac{P_{ext}}{P_{\text{int}}}\right)^{\frac{\gamma+1}{\gamma}} \right]} \quad (2)$$

$$P_L = 1.6 \cdot 10^{12} \times \frac{Q_T^{1.85} L}{d_p^5 P_I} \quad (3)$$

$$P_R = \frac{\rho_{int}}{2\left(V_i^2 - V_f^2\right)} \quad (4)$$

Where:

Q_n = Flow rate through the orifice under atmospheric conditions (1 atmosphere and 20 °C), m_n^3/s
ρ_{atm} = Air density at atmospheric conditions (ρ_n = 1.19 kg/m^3 at 1 atmosphere and 20 °C)
C = Coefficient of discharge, unitless
A = Total area of nozzles in source cluster, m^2
ρ_{int} = Air density at the source cluster, inside the diffuser, kg/m^3
γ = Heat capacity ratio ($\gamma = 1.4$ for air), unitless
P_{int} = Absolute pressure at the source cluster, inside the diffuser, Pa
P_{ext} = Absolute pressure outside the source cluster (hydrostatic pressure from water depth), Pa
P_L = Pressure loss in a straight compressed air delivery pipeline, kPa
Q_T = Total free air flow rate, m^3/s
d_p = Inner diameter of the pipe, mm
L = Total length of the pipe, including fittings, etc., m
P_I = Absolute initial line pressure, kPa
P_R = Pressure recharge, Pa
V_i = Air flow velocity just upstream of a source cluster, m/s
V_f = Air flow velocity just downstream of a source cluster, m/s

The experimental results of this study (Figure 4) show that Equation (2) was a good fit over the range of experimental data: nozzle diameters from 1.5 to 7 mm and flow rates from 2 to 20 L_n/s. Equation (2) applies to subcritical flow conditions, which occurs when the pressure inside the diffuser is less than 1.9 times the pressure outside the diffuser.

The flow conditions through the Pindari diffuser design were checked for the reservoir conditions most likely to cause super critical flow: using the historic low water level of 463 m AHD (meaning the lowest external hydrostatic pressure), and requiring 1000 L/s total air flow (the maximum design airflow rate, meaning the greatest internal pressure). The ratio of $P_{\text{int}}/P_{\text{ext}}$ was 1.7 under these worst case conditions, confirming that the Pindari diffuser will always have subcritical flow conditions. It should also be noted that these conditions are unlikely to occur during operations as a much lower air flow rate would be required to destratify the near empty reservoir.

4.3 Nozzle efficiency

For a given pressure condition, the head loss through a nozzle can be affected by the coefficient of discharge or the port diameter. The coefficient of discharge could be increased by using engineered nozzles with more efficient nozzles, however this comes with increased cost and construction complexity. Instead, the same increase in flow through a nozzle could be achieved by simply increasing the port diameter, which comes at no extra cost or complexity. As such, drilled hole nozzles are recommended over engineered nozzles.

Additionally, WRL's design approach was to ensure that the losses along the diffuser pipeline were relatively small compared to the losses through the nozzles. This approach was to ensure that the airflow distribution along the diffuser was approximately uniform, preventing all the air from flowing out the first few source clusters. If the nozzles are too large and the losses are too low, then all the air will flow out of the first source cluster, resulting in a poor distribution. If the pipeline is too small and has excessive friction losses, then the interior pressure difference between source clusters will be large and thus the first diffusers will have more flow than the later clusters, resulting in a poor distribution.

WRL's design has also adopted larger hole diameters than the 1 to 1.5 mm diameter previously recommended by Wuest et al. (1992) for bubble plume destratification systems. This was in light of more recent research finding that the size of the nozzle diameter above 1 mm has negligible impact on the slip velocity between the bubbles and the surrounding water (Park et al., 2017). Further, the intention of this design was to aerate the reservoir through mixing and breaking the stratification, not dissolving oxygen into the lower reservoir.

4.4 Sensitivity of design

4.4.1 Coefficient of discharge

The coefficient of discharge determined in this study was 0.68 ± 0.05 for a 5 mm hole, slightly higher than the 0.62 value which was assumed in the design of the diffuser. As such, the design calculations were repeated with the new coefficient and the upper and lower limits to assess impacts on the diffuser design. Sensitivity analysis showed that a ± 0.05 change in the coefficient of discharge had a negligible impact on the diffuser performance. The impact on required compressor pressure is shown in Table 4 and was found to be negligible. No difference was observed between the previous coefficient value (0.62) and the new lower value (0.63). The change in air flow distribution along the diffuser pipeline due to the coefficient of discharge was also assessed and found to have minimal impact, see Figure 6. The impact on the distribution was assessed over a design envelope for Pindari, with air flow rates ranging from 300 to 1000 L/s and water depths above the diffuser pipeline varying from 30 to 70 m (based on historic low water levels).

Table 4 Effect of coefficient of discharge on required compressor pressure

Coefficient of discharge	Flow rate (L/s)	Compressor pressure (bar) at different water levels above the diffuser				
		70 m	60 m	50 m	40 m	30 m
0.63	300	8.0	7.0	6.0	5.1	4.1
0.68	300	7.9	7.0	6.0	5.1	4.1
0.73	300	7.9	7.0	6.0	5.0	4.1
0.63	600	8.2	7.2	6.3	5.4	4.5
0.68	600	8.1	7.2	6.3	5.4	4.5
0.73	600	8.1	7.2	6.3	5.3	4.5
0.63	1000	8.6	7.8	6.9	6.1	5.4
0.68	1000	8.6	7.7	6.8	6.0	5.3
0.73	1000	8.5	7.6	6.8	6.0	5.2

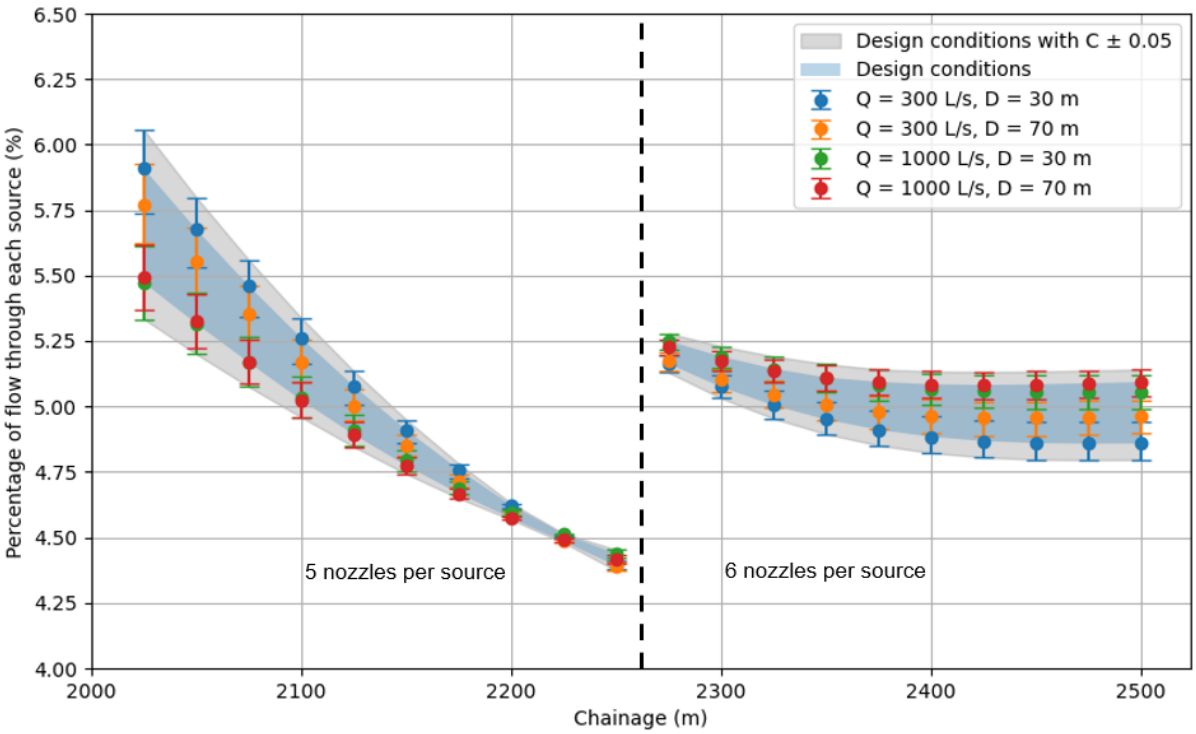

Figure 6 Impact of variability of coefficient of discharge on flow distribution along diffuser pipeline. The dashed black line indicates the change in the number of nozzles per source.

4.4.2 Port diameter

During experimentation, it was noticed that the diameter of the drilled holes did not match the expected value, resulting in an observable difference in air flow through the holes. As such, design calculations were repeated with the port diameter changed by ± 0.5 mm to assess the sensitivity of the Pindari diffuser design to port diameter. Sensitivity analysis showed that a ± 0.5 mm change in port diameter was found to have a negligible impact on diffuser performance. The impact on required compressor pressure is shown in Table 5, and the change in pressure distribution along the pipeline was found to be minimal, see Figure 7.

Table 5 Effect of port diameter on required compressor pressure

Diameter (mm)	Flow rate (L/s)	Compressor pressure (bar) at different depths				
		70 m	60 m	50 m	40 m	30 m
4.5	300	8.0	7.0	6.0	5.1	4.1
5.0	300	7.9	7.0	6.0	5.1	4.1
5.5	300	7.9	7.0	6.0	5.0	4.1
4.5	600	8.2	7.3	6.4	5.5	4.6
5.0	600	8.1	7.2	6.3	5.4	4.5
5.5	600	8.1	7.2	6.2	5.3	4.4
4.5	1000	8.8	7.9	7.1	6.3	5.6
5.0	1000	8.6	7.7	6.8	6.0	5.3
5.5	1000	8.5	7.6	6.7	5.9	5.1

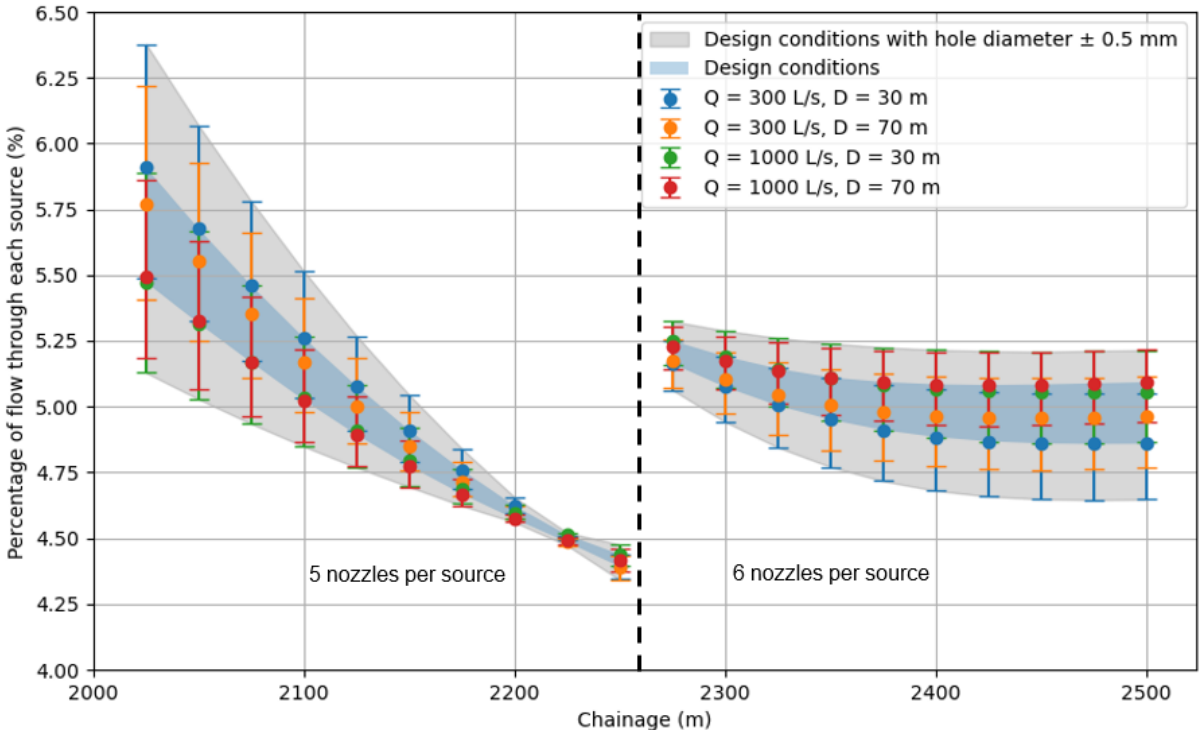

Figure 7 Impact of variability of port diameter on flow distribution along diffuser pipeline. The dashed black line indicates the change in the number of nozzles per source.

5 Conclusion

This report presents laboratory testing of pneumatic air flow into a water column through various diffuser port sizes. Tested diffuser port sizes, air flow rates and pressure were selected to capture the range of values expected to be used in a bubble plume destratification system. This study aimed to validate the theoretical equations for air flow through a diffuser port, and determine both the value and variability of the coefficient of discharge.

- The existing theory fit the experimental data very well, with a coefficient of determination (R^2) value of 0.995.
- The coefficient of discharge was found to be 0.68 ± 0.05 for a 20 mm thick HDPE plate.
- A major source of variation in the coefficient of discharge was the tolerance for diffuser hole sizes.

The implications of these experimental results on the Pindari dam diffuser design were also assessed. Based on the validated theoretical equations and WRL's design approach, drilled hole nozzles were found to be more suitable than engineered nozzles. This is because the benefit of the more efficient engineered nozzle can simply be achieved by drilling more hole nozzles at no extra cost. Furthermore, the measured variability in coefficient of discharge (± 0.05) and expected variability in diffuser port diameter (± 0.5 mm) were found to have a negligible impact on the Pindari diffuser design.

6 References

Chaaya, F. C. and Miller, B. M. (2022) A review of artificial destratification techniques for cold water pollution mitigation A review of artificial destratification techniques for cold water pollution mitigation, WRL Technical Report 2021/017, UNSW Water Research Laboratory.

Chaaya, F C and Miller, B M (2023a), Pindari dam – mitigating cold water pollution through artificial destratification, WRL Technical Report 2022/04, UNSW Water Research Laboratory.

Chaaya, F C and Miller, B M (2023b), Pindari Dam cold water pollution mitigation through artificial destratification – Monitoring network recommendations, WRL Technical Report 2022/19, UNSW Water Research Laboratory.

Chaaya, F C and Miller, B M (2024a), Pindari destratification trial – conceptual pneumatics design, WRL Technical Report 2023/05, UNSW Water Research Laboratory.

Chaaya, F C and Miller, B M (2024b), Pindari destratification – numerical modelling of operational procedures to balance power requirements, WRL Technical Report 2024/05, UNSW Water Research Laboratory.

Lewis, D. P., Patterson, J. C., Imberger, J., Wright, R. P. and Schladow, S. G. (1991) Modelling and Design of Bubble Plume Destratification Urban Water Research Association of Australia

Sung Hoon Park, Changhwan Park, JinYong Lee, Byungchul Lee, 2017. A Simple Parameterization for the Rising Velocity of Bubbles in a Liquid Pool, Nuclear Engineering and Technology, Volume 49, Issue 4, 1738-5733.

U.S. Federal Emergency Management Agency (FEMA), U.S. Dept. of Transportation (DOT), and U.S. Environmental Protection Agency (EPA), 1989. Handbook of Chemical Hazard Analysis Procedures. Washington, DC.

Wuest, A, Brooks, N H and Imboden, D M, 1992. Bubble plume modelling for lake restoration, *Water Resour. Res.*, 28(12), 3235–3250, doi:10.1029/92WR01681.

Appendix A Full experimental results

Full results for each scenario and test are provided in Table A-1. Values of the best fit C (coefficient of discharge) for each test were determined by finding the single C value that minimised the root mean square error (RMSE) for each individual test timeseries (1 minute timeseries with flow and pressures sampled every second).

Table A-1 Complete experimental results

Scenario ID	Test number	Arrangement	Average P_{int} (kPa)	Average P_{ext} (kPa)	Measured flow (L_n/s)	Best fit C for each test
S1	T01	4 x 1.5 mm holes	1.52	1.04	1.70	0.75
S1	T02	4 x 1.5 mm holes	1.75	1.06	2.05	0.74
S1	T03	4 x 1.5 mm holes	1.99	1.07	2.37	0.75
S1	T04	4 x 1.5 mm holes	1.98	1.50	1.81	0.71
S1	T05	4 x 1.5 mm holes	2.24	1.51	2.29	0.74
S1	T06	4 x 1.5 mm holes	2.57	1.52	2.90	0.78
S1	T07	4 x 1.5 mm holes	2.96	2.02	2.97	0.76
S1	T08	4 x 1.5 mm holes	3.01	2.48	2.19	0.69
S1	T09	4 x 1.5 mm holes	3.22	2.52	2.56	0.70
S1	T10	4 x 1.5 mm holes	2.75	2.02	2.45	0.72
S1	T11	4 x 1.5 mm holes	2.51	2.00	1.99	0.69
S2	T01	1 x 3 mm hole	2.00	1.06	2.10	0.66
S2	T02	1 x 3 mm hole	1.49	1.03	1.53	0.69
S2	T03	1 x 3 mm hole	1.76	1.05	1.77	0.64
S2	T04	1 x 3 mm hole	2.52	1.49	2.27	0.62
S2	T05	1 x 3 mm hole	2.72	1.50	2.45	0.61
S2	T06	1 x 3 mm hole	2.98	1.50	2.87	0.65
S2	T07	1 x 3 mm hole	3.02	2.02	2.63	0.66
S2	T08	1 x 3 mm hole	3.02	2.49	1.88	0.60
S2	T09	1 x 3 mm hole	3.24	2.51	2.21	0.60

Scenario ID	Test number	Arrangement	Average P_{int} (kPa)	Average P_{ext} (kPa)	Measured flow (L_n/s)	Best fit C for each test
S2	T10	1 x 3 mm hole	3.50	2.54	2.49	0.58
S3	T01	1 x 3 mm hole burred	1.97	0.99	2.88	0.74
S3	T02	1 x 3 mm hole burred	1.51	0.96	2.22	0.76
S3	T03	1 x 3 mm hole burred	1.67	0.97	2.45	0.74
S3	T04	1 x 3 mm hole burred	2.48	1.53	3.28	0.75
S3	T05	1 x 3 mm hole burred	2.00	1.54	2.33	0.76
S3	T06	1 x 3 mm hole burred	2.25	1.56	2.70	0.72
S3	T07	1 x 3 mm hole burred	2.50	2.00	2.43	0.70
S3	T08	1 x 3 mm hole burred	2.86	2.01	3.42	0.76
S3	T09	1 x 3 mm hole burred	3.00	2.53	2.47	0.67
S4	T01	5 x 3 mm hole burred	1.49	1.00	8.14	0.64
S4	T02	5 x 3 mm hole burred	1.76	1.00	10.34	0.66
S4	T03	5 x 3 mm hole burred	2.01	1.00	12.22	0.68
S4	T04	5 x 3 mm hole burred	2.50	1.49	13.51	0.67
S4	T05	5 x 3 mm hole burred	2.75	1.49	15.43	0.69
S4	T06	5 x 3 mm hole burred	2.99	1.50	16.78	0.69
S4	T07	5 x 3 mm hole burred	2.99	2.01	14.66	0.67
S4	T08	5 x 3 mm hole burred	3.28	2.01	16.81	0.68
S4	T09	5 x 3 mm hole burred	3.45	2.00	17.62	0.67
S4	T10	5 x 3 mm hole burred	3.50	2.51	15.96	0.67
S4	T11	5 x 3 mm hole burred	3.69	2.51	17.32	0.67
S5	T01	1 x 5 mm hole	1.51	1.00	4.49	0.64
S5	T02	1 x 5 mm hole	1.75	1.03	5.53	0.65
S5	T03	1 x 5 mm hole	2.00	1.04	6.22	0.64
S5	T04	1 x 5 mm hole	2.51	1.50	7.88	0.71
S5	T05	1 x 5 mm hole	2.75	1.51	8.60	0.70
S5	T06	1 x 5 mm hole	3.03	1.53	9.47	0.70
S5	T07	1 x 5 mm hole	3.49	2.03	10.09	0.69
S5	T08	1 x 5 mm hole	3.74	2.04	11.02	0.70
S5	T09	1 x 5 mm hole	4.01	2.03	12.04	0.71

Scenario ID	Test number	Arrangement	Average P_{int} (kPa)	Average P_{ext} (kPa)	Measured flow (L_n/s)	Best fit C for each test
S5	T10	1 x 5 mm hole	4.58	2.52	13.13	0.70
S5	T11	1 x 5 mm hole	4.81	2.53	13.96	0.71
S5	T12	1 x 5 mm hole	5.15	2.48	15.75	0.75
S6	T01	1 x 7 mm hole	1.50	0.99	8.91	0.62
S6	T02	1 x 7 mm hole	1.74	1.00	11.30	0.65
S6	T03	1 x 7 mm hole	2.03	1.01	13.44	0.66
S6	T04	1 x 7 mm hole	2.55	1.49	15.42	0.67
S6	T05	1 x 7 mm hole	2.79	1.49	16.96	0.66
S6	T06	1 x 7 mm hole	2.94	1.49	18.00	0.67
S6	T07	1 x 7 mm hole	3.06	2.01	16.93	0.67
S6	T08	1 x 7 mm hole	3.15	2.01	18.69	0.70
S6	T09	1 x 7 mm hole	3.50*	2.01	*	*
S6	T10	1 x 7 mm hole	2.74	2.02	13.59	0.64

* Compressor could not achieve this pressure.